SLAC–PUB–5157
IUHEE–89–2
December 1989
(E/I)

TRACKING WITH WIRE CHAMBERS AT HIGH LUMINOSITIES*

GAIL G. HANSON
Indiana University, Bloomington, Indiana 47405 USA
and
Stanford Linear Accelerator Center, Stanford University,
Stanford, California 94309, USA

Abstract

Radiation damage and rate limitations impose severe constraints on wire chambers at the SSC. Possible conceptual designs for wire chamber tracking systems that satisfy these constraints are discussed. Computer simulation studies of tracking in such systems are presented. Simulations of events from interesting physics at the SSC, including hits from minimum bias background events, are examined. Results of some preliminary pattern recognition studies are given.

1. Introduction

The primary motivation for the SSC is the expectation that it will lead to new discoveries, such as Higgs bosons, supersymmetric particles, heavy W's or Z's, new heavy fermions, or composite particles with masses in the TeV region. Such particles would be produced in the central rapidity region, that is, over $\pm$ 3 units of rapidity, and would decay to high-p_T electrons, muons, or jets, often with large missing transverse energy due to undetectable neutrinos. In order to fully investigate the physics opportunities in this regime, a general-purpose detector which includes charged particle tracking is needed.

Tracking at the SSC at the full design luminosity, $\mathcal{L}$, of 10^{33} cm^{-2}s^{-1} is expected to be a difficult problem. The limitations imposed by rates and radiation damage have been described by the previous speaker [1]. Once the wire chambers can be shown to survive, the dominant constraint is the combination of occupancy and double-hit resolution. Single events from new physics at the SSC have many (several hundred) charged particle tracks and are further complicated by curling tracks in a magnetic field, photon conversions, hits from events from out-of-time bunch crossings, and multiple interactions within the same bunch crossing [2]. We have begun studies using computer simulation to establish how well one can find tracks in complex SSC events.

* Work supported by the Department of Energy, contracts DE–AC03–84ER40125 and DE–AC03–76SF00515.

Invited talk presented at the ECFA Study Week on Instrumentation Technology for High Luminosity Hadron Colliders, Barcelona, Spain, September 14–21, 1989

2. Wire Chamber Requirements

2.1. Constraints of the SSC Environment on Cell Design

Limitations on wire chamber tracking detectors at the SSC are imposed by radiation damage, current draw, chamber lifetime, gain reduction from large particle flux, hit rate, occupancy and pattern recognition. Of these, the most severe is probably current draw since this determines survivability in the SSC environment. For wires parallel to the beam direction in a central tracking system, current draw per wire, I, for a layer of wires of length L at radius r is given by

$$I = \frac{n_c w h \sigma \mathcal{L} G e \alpha L}{2 \pi r^2} \quad , \tag{1}$$

where n_c is the average charged particle multiplicity per unit of rapidity (7.5), w and h are the width and height of the cell (assumed to be equal), e is the electron charge, and σ is the inelastic cross section (100 mb). The ionization rate, α, in the gas is assumed to be 100 electrons/cm, and the gas gain, G, is assumed to be 2×10^4, which is rather low. A layer of 4 mm wide cells at a radius of 50 cm covering $|\eta| < 1.5$ ($L = 213$ cm) will draw 0.52 μA/wire. The limit of acceptable current draw before breakdown will occur is about 1 μA/wire. For the above example, the collected charge over a chamber lifetime of five years (5×10^7 s) would be 0.12 C/cm, where the limit is about 1.0 C/cm. However, this calculation includes only the particles produced in an interaction and must be increased by a factor of 2–4 because of curling tracks in a magnetic field, converted photons, and albedo particles leaking out of the front face of the calorimeter. An extra safety margin may be obtained by splitting the length of wire needed to cover the entire rapidity range in the middle or increasing the minimum radius at which the tracking system operates at the full design luminosity.

Straw tube chambers are a natural candidate for a small cell design. The straws are typically made of aluminized polyester film (Mylar) or polycarbonate (Lexan) with wall thicknesses of about 30 μm. Several layers of straw tubes can be glued together to form superlayers which would be rigid, mechanically stable structures. Within each superlayer the layers can be staggered by half the cell width in order to allow hits from out-of-time bunch crossings to be rejected and resolve left-right ambiguities, as illustrated in fig. 1. By dividing the chamber into superlayers, locally identifiable track segments can be obtained at the pattern recognition stage. The track segments can then be linked to form tracks. There must be a sufficient number of layers in the superlayers to provide redundancy.

Since cell widths are constrained to a few mm, vector cells (jet cells) in the central tracking region are not practical. However, in the forward tracking region ($|\eta| \gtrsim 1.5$), the radial wire chamber may be an excellent candidate [1, 3]. The current draw per

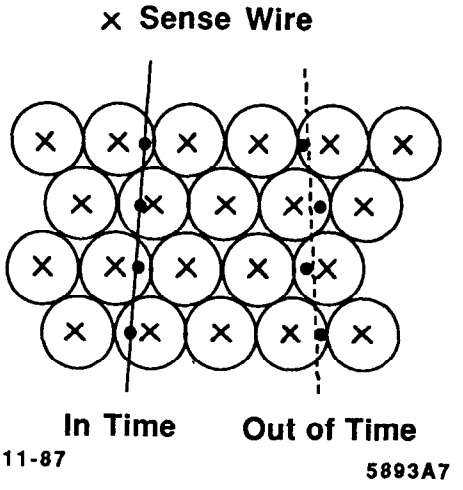

Fig. 1. Layers of straw tubes in a superlayer with every other layer staggered by the straw tube radius. A single in-time track will appear as a series of hits on the wires on alternate sides of the track. The left-right ambiguity is easily resolved locally. A track from an out-of-time bunch crossing will produce hits which are displaced from possible tracks by at least 16 ns in drift time.

wire for a radial wire chamber is given by

$$\frac{d^2Q}{dr\ dt} = \frac{n_c \sigma \mathcal{L} G e \alpha h}{r N_{cell}} \quad , \tag{2}$$

where h is the distance between sense wires in a wedge and N_{cell} is the number of wedges azimuthally. The current draw is inversely proportional to the radial position along the wire. For $h = 4$ mm and 335 wedges, the current draw is $(2.9 \times 10^{-7}$ C/s)/ r(cm), which integrates to 0.3 C/cm/5 years at a radial position of 50 cm. For a radial wire chamber there is no increase in current due to curling tracks in a magnetic field.

Other possible problems for wire chambers at the SSC were considered at the Vancouver SSC Tracking Workshop [4]. Space charge effects should not be a problem for straw tube chambers because the drift distance is so small and are probably not a problem for radial wire chambers. The current draw causes about 1 mW of power dissipation in the gas of a single straw, but this can probably be handled by adequate gas flow. The neutron and photon albedo were estimated to increase the current draw by about 20%. The calculation should be done more carefully, and we should also look at the effects for existing tracking chambers in front of calorimeters.

2.2. Measurement of the Coordinate Along the Wire

The three conventional methods for measuring the coordinate along a wire are charge division, small-angle stereo, and cathode strips (or pads) running perpendicular to the wires. A fourth, less conventional, method is the time-difference method which probably has similar resolution to charge division, but may be worth further consideration.

Charge division, at best (high gas gain $\sim 10^5$), gives a resolution of about 1% of the length of the wire. Since the wires in an SSC tracking system would be quite long (3–6 m) in order to cover the required rapidity range, the resolution would be only 3–6 cm. Since low gas gain is needed to reduce current draw and increase chamber lifetime, the resolution in an SSC tracking system would be even worse. Also, charge division requires electronics readout at both ends of the wire which increases the complexity of a system with a large number of wires. For these reasons charge division does not appear to be a practical method for measuring the coordinate along the wire in an SSC tracking system.

Small-angle stereo ($\sim 3°$) wires typically give a resolution in the coordinate along the wire of a few mm (the drift distance resolution divided by the stereo angle). The same electronics for time measurement can be used for all wires. In a system of superlayers of straw tubes, every other superlayer might be small-angle stereo. However, in complex SSC events it may be difficult to associate the hits on stereo wires with the correct tracks. The H1 radial wire chambers use charge division plus planes of crossed wires to resolve ambiguities. For the SSC, "stereo" wires at a small angle to radial may work to determine the coordinate along the radial direction.

Cathode strips or pads perpendicular to the wire direction can give a resolution of better than 1 mm. They might be included on the outer surfaces of the superlayers in the central tracking system to aid in bunch assignment and reducing stereo ambiguities and in front of the calorimeter in the forward tracking system. However, they present added electrical and mechanical difficulties, as well as increasing the number of readout channels.

2.3. Momentum Measurement

The minimum requirement for momentum resolution based on physics criteria is that the sign of the charge for electrons should be measured for $p_T \leq 0.5$–1.0 TeV/c, or $\sigma_{p_T}/p_T \leq 0.30 p_T$ (TeV/c). To obtain this momentum resolution in a robust manner, one can scale from existing detectors, such as Mark II and CDF. One then finds that for a magnetic field of 2 Tesla and a tracking inner radius of 50 cm, we need an outer radius of about 1.8 m to obtain the required momentum resolution for non-beam-constrained momentum fits. It has been found that the momentum resolution is generally worse than the ideal due to systematic errors in positioning, imperfect pattern recognition, and lost hits in complex events in large tracking systems. Of course, we would really like to achieve better than the minimum requirement for

momentum resolution, for example, in order to reconstruct invariant masses involving high-momentum muons. We can improve on the above momentum resolution by using beam-constrained fits where appropriate, trying to improve the spatial resolution for the large tracking system, and by including a few layers of silicon detectors with very precise spatial resolution at small radius inside the wire chamber system. Such silicon systems still require considerable R&D to show that they will work reliably in the SSC environment and achieve the calculated momentum precision.

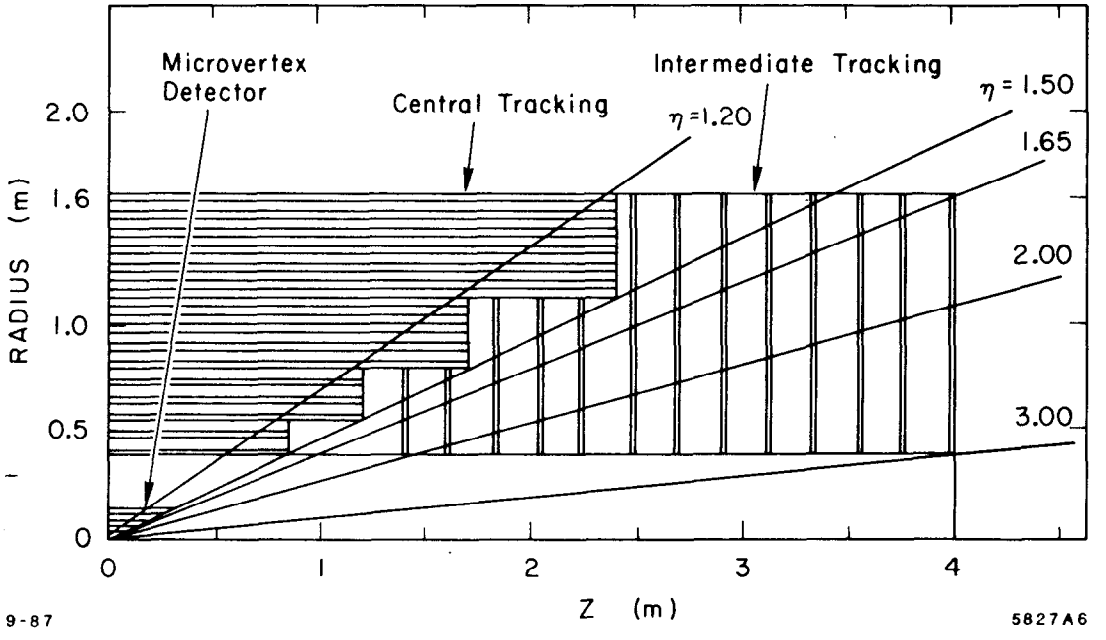

Fig. 2. Schematic view of the central and intermediate tracking systems in the Large Solenoid Detector (from ref. [5]).

2.4. Examples of SSC Tracking Systems

A large solenoid detector based on more-or-less "conventional" technology was discussed at the 1987 Berkeley Workshop [5]. Calorimetry and tracking are located inside a large superconducting solenoid with 2 Tesla field. The tracking detector design for the Large Solenoid Detector was divided into central tracking ($|\eta| \lesssim 1.2$) and intermediate tracking ($1.2 \lesssim |\eta| < 2.5$). The central tracking system was assumed to be built of superlayers of straw tubes of radii from 2 to 3.5 mm parallel or nearly parallel to the beam direction. Every other superlayer is small-angle stereo. Two options for intermediate tracking were considered: planes of parallel wires and radial wire chambers. A schematic view of the tracking system in the Large Solenoid Detector is shown in fig. 2.

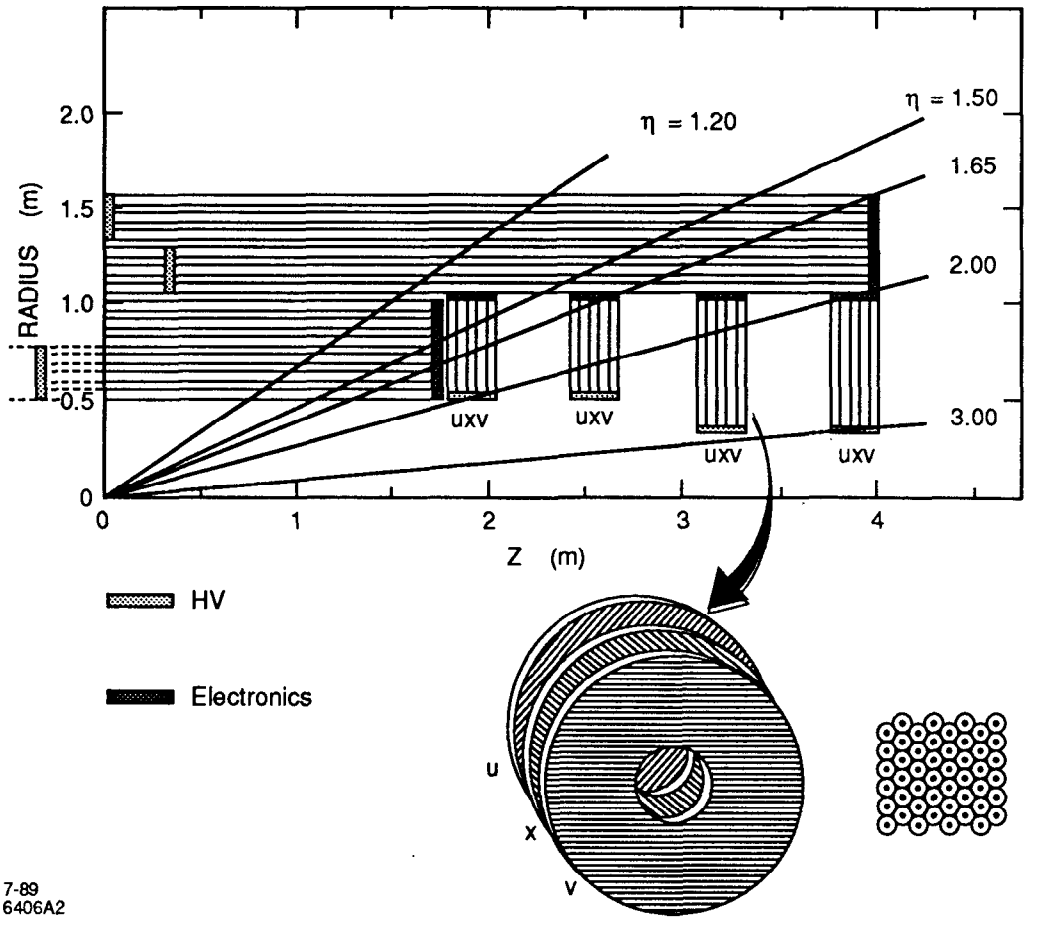

Fig. 3. Schematic view of a solenoidal detector tracking system capable of measuring p_T in the outer superlayers for $|\eta| \lesssim 2$. The tracking system for $2 < |\eta| < 3$ consists of planar superlayers of straw tubes.

In a solenoidal detector with geometry as in the Large Solenoid Detector, the momentum resolution becomes very large near $|\eta| \sim 2$, so in reality one can hope to measure only track positions at the entrance to the calorimeters for larger $|\eta|$. On the other hand, one can use the outer superlayers to measure p_T, for example, for the trigger, for $|\eta| \lesssim 2$. In principle (see sec. 3.3), we know how to do this for wires parallel to the beam direction. This leads to the idea of extending the axial wires to cover this area. Also, position measurement for $2 < |\eta| < 3$ can be accomplished with planar superlayers of straw tubes. Track segments can be found in the superlayers in a manner similar to the central tracking. The wires in these superlayers would run alternately at $\pm$ 45° to each other (u, x, v). A tracking system incorporating these

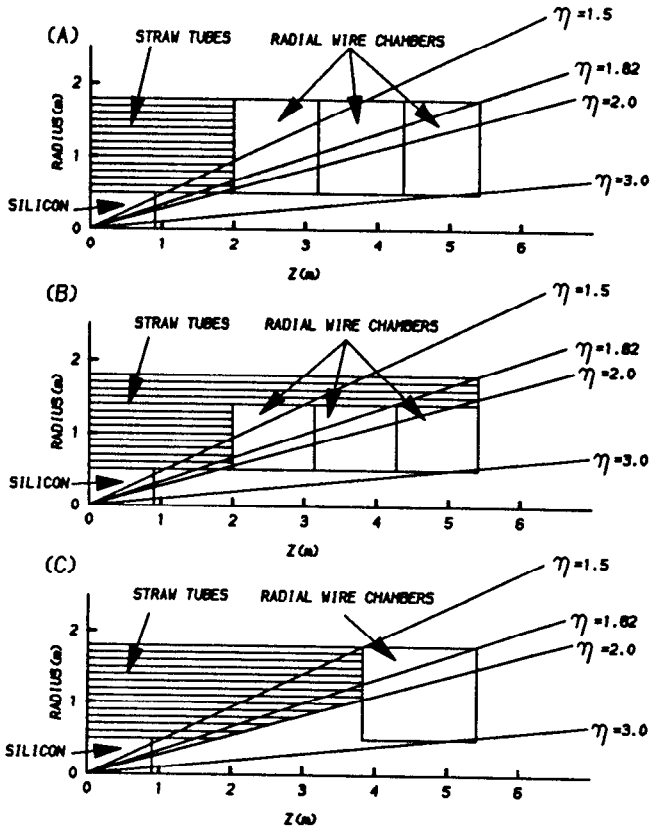

Fig. 4. Various options for combining central tracking with radial wire chamber modules. All have 50 cm inner radius, 180 cm outer radius and length sufficient to cover $|\eta| < 1.82$ with all tracking layers and $|\eta| < 2.0$ with momentum resolution degraded by no more than about a factor of two. (a) Axial wires covering $|z| < 2.0$ m and radial wire chambers covering $|z| > 2$ m. (b) Axial wires covering $|\eta| < 2.0$ in order to find high-p_T track segments for the trigger. (c) Tracks cross only one boundary between central and forward tracking, except at $|\eta| = 2.0$.

ideas is shown in fig. 3.

Figure 4 shows three options for combining central tracking with radial wire chamber modules for forward tracking. We would like to be able to construct high-p_T track segments for the trigger. If we can understand how to accomplish this with radial wires, then the tracking systems shown in figs. 4(a) or (c) would be preferable because they do not require such long wires.

3. TRACKING SIMULATION

3.1. Simulation of a Central Tracking System for the SSC

The SSC tracking system design used for this simulation was based on that for the Large Solenoid Detector [5], described in sec. 2.4, although it is quite general and can be used for any system of cylindrically oriented sensing elements. The simulation has been described in detail elsewhere [6–9]. Briefly, we used ISAJET [10] to generate events from interesting physics processes, such as high-p_T two-jet events or Higgs boson production, and from inelastic scattering background, for which we used minimum bias events. We used the GEANT3 [11] general-purpose detector simulation package to simulate the interactions of the particles with the detector. The particles interact in the 8% of a radiation length of material due to straw tube walls, wires, and gas (the material was assumed to be distributed uniformly throughout the tracking volume), including photon conversion and multiple Coulomb scattering. The digitizations consist of a wire number and a drift time, calculated from the distance of closest approach of a track to a wire using a drift velocity of 50 μm/ns, for each track in each layer. Background from inelastic scatterings in the same and out-of-time bunch crossings is included by superimposing the digitizations from minimum bias events from the number of bunch crossings as determined by the resolving time of the straw tube cell. The double-hit resolution is equal to the cell width, that is, only the earliest hit on a wire is kept.

3.2. Results of the Simulation

Figure 5(a) shows a simulation of a two-jet event with $p_T > 1$ TeV/c in the Large Solenoid Detector, and fig. 5(b) shows an enlargement of the same event in the outer two superlayers in the area of the dense jet. Figure 5(c) shows the earliest hits in the cells for the tracks shown in fig. 5(b). Hits from background events and converted photons are not shown in fig. 5.

Figure 6 shows the same event as in fig. 5, but with no magnetic field. In figs. 5 and 6 we can observe that the hits form identifiable tracks in the outer superlayers with a 2 Tesla field, but with no magnetic field the tracks are less easily resolved. The 2 T field, however, produces many curling tracks which obscure the high-p_T tracks to some extent, particularly in the inner superlayers.

Figure 7 shows an event from Higgs boson production, $pp \rightarrow HX$, with the Higgs decaying to Z^0Z^0 and each Z^0 decaying to e^+e^- or $\mu^+\mu^-$. We used a Higgs mass of 400 GeV/c^2. For these events we used the full simulation as described in the previous section. We generated $\sim$ 200 such events, which we used for further studies of hit loss and pattern recognition.

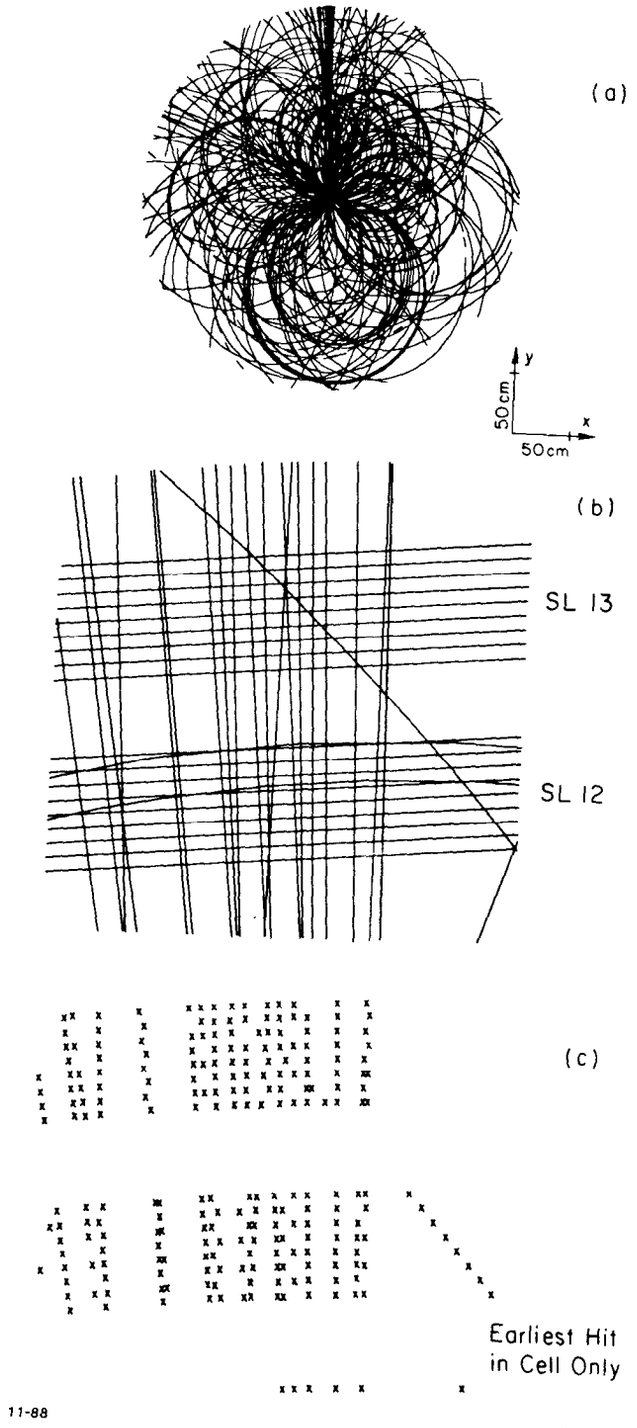

Fig. 5. (a) Two-jet event from ISAJET with $p_T > 1$ TeV/c in a 2 Tesla magnetic field in a detector of the geometry of the Large Solenoid Detector. There are 223 particles with $p_T > 200$ MeV/c and $|\eta| < 1.5$. Converted photons and background from minimum bias events are not shown. (b) Enlargement of the event in the outer two superlayers in the area of the dense jet at the top of the detector. (c) Earliest hit in each cell for the tracks shown in (b).

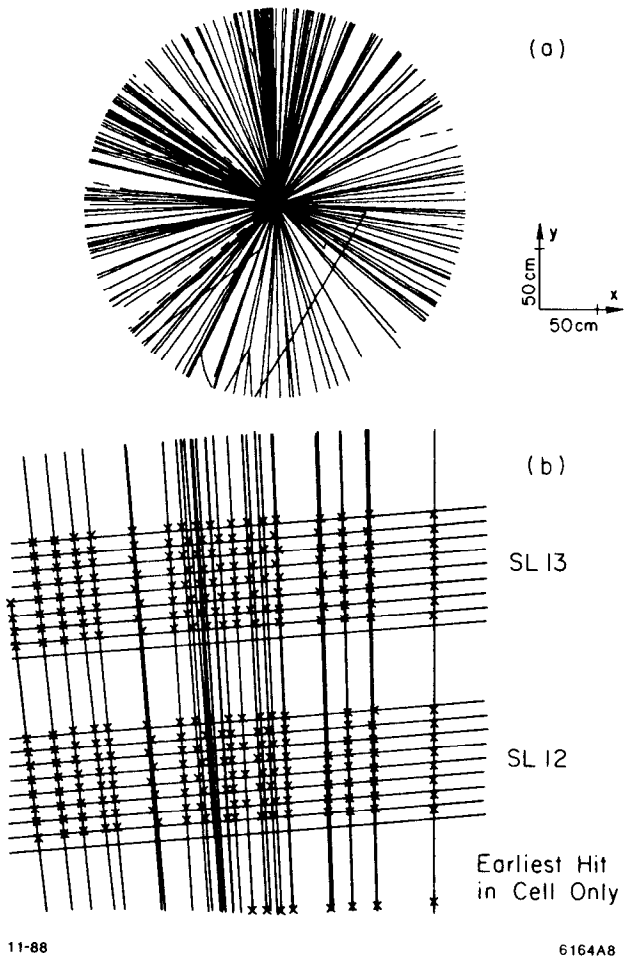

Fig. 6. (a) Same two-jet event from ISAJET as shown in fig. 5, except with no magnetic field. (b) Tracks and earliest hit in each cell in the enlargement of the event in the outer two superlayers in the area of the dense jet at the top of the detector.

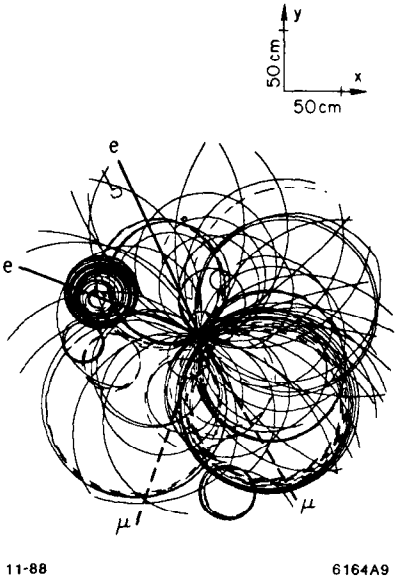

Fig. 7. Example of a Higgs event in the simulated central tracking system. The leptons from the Higgs decay are indicated by the heavier lines. Converted photons and other interactions with the material are included.

The fully-simulated events, including adding digitizations from minimum bias background events and removing digitizations within the double-hit resolution, had 12,000 – 30,000 digitizations in the central tracking system. On the average 57% of the digitizations were due to minimum bias background events. For all tracks $(11.6 \pm 0.7)\%$ of the digitizations were lost because of the double-hit resolution, and the loss was about the same in all superlayers. For the leptons from the Higgs decay an average of $(7.3 \pm 0.6)\%$ of the digitizations were lost with the worst losses being in the inner superlayers.

We are now beginning to include intermediate tracking in the simulation. Figure 8 shows a projection in the direction along the beam line of a simulated Higgs event in a detector similar to that shown in fig. 3.

3.3. Pattern Recognition

We began working on pattern recognition algorithms in order to examine our original design goals of finding track segments in superlayers and removing hits from out-of-time bunch crossings. The algorithm for finding track segments was the following:

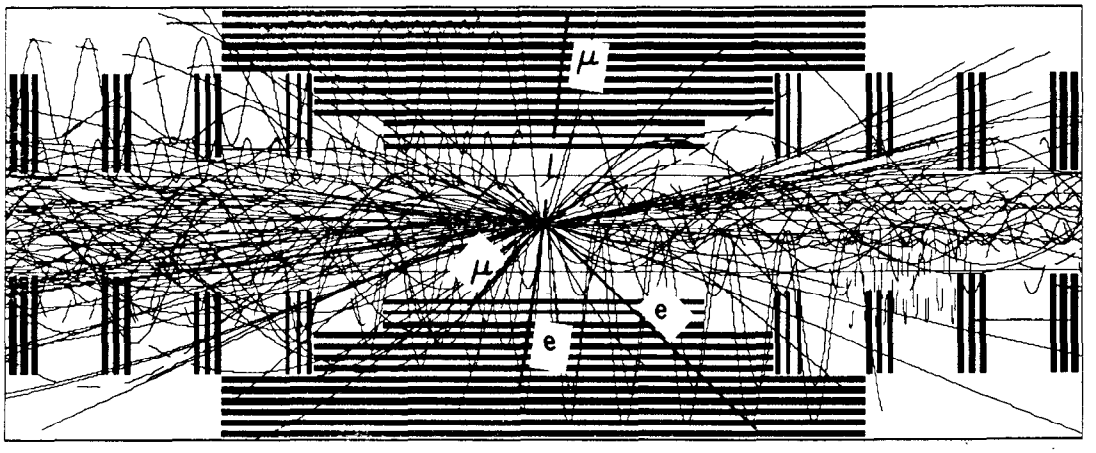

Fig. 8. Example of a Higgs event in a projection along the beam direction. The central tracking system is the same as that shown in fig. 2 and the intermediate tracking system is that shown in fig. 3. The leptons from the Higgs decay are indicated by the heavier lines. Converted photons and other interactions with the material are included.

1. In each superlayer we identified "roads" containing hits. There are two parameters which can be varied: the width of the road and the number of hits required on the road. We used a width of five wires and required three or more hits out of eight possible.

2. We required that at least one of the hits be in a layer with the opposite wire stagger from the others so that the left-right ambiguities could be resolved.

3. We required that the hits be consistent with a straight line to within an error based on the spatial resolution and in the process resolved the left-right ambiguities.

Figure 9(a) shows all of the digitizations for the event shown in fig. 7, including those from minimum bias background events. Figure 9(b) shows only those digitizations which are included in segments. Keeping only those digitizations which form segments cleans up the events considerably. Figure 9(c) shows the tracks from the original event in the outer five superlayers in the region around the muon at the lower right. Figure 9(d) shows all of the digitizations in the event in the enlarged region (the digitizations are displayed at the locations of the hit wires). Finally, fig. 9(e)

shows only those digitizations which form track segments; here, the left-right ambiguities have been resolved, the drift times have been converted to distances, and the digitizations are displayed at the positions of closest approach of the tracks to the wires. One can clearly identify the muon track, and most of the extra hits have been removed.

Next, we applied our segment-finding algorithm to the e and μ tracks from Higgs boson decays. We defined two classes of segments: a "good" segment was one with at least five hits from a lepton track and no other hits, and an "OK" segment was one with at least five hits from the lepton track and one hit from another track. The effects of hits from other tracks remain to be studied; we plan to compare measured momenta with produced momenta in future work. With these definitions, we counted the number of segments found for each lepton track.

The distribution of the number of good segments for the e's and μ's in the Higgs events is shown in fig. 10(a). The corresponding distribution of total (good or OK) segments is shown in fig. 10(b). We see that the lepton tracks from Higgs decay have an average of about 8 good segments and 10 total segments out of 13 possible. Typically 30–50% of segments were good in the inner superlayers, increasing to almost 80% for the outer superlayers. When OK segments are counted as well, 50–60% of segments are accepted for inner superlayers and over 80% for outer superlayers.

After finding the hits in roads, we can find the coordinate along the wire from the displacement of nearby axial and stereo roads. We can then correct the drift times for the propagation time along the wires and determine the bunch number from the time offset which gives a straight line. We will test this procedure in future simulation work.

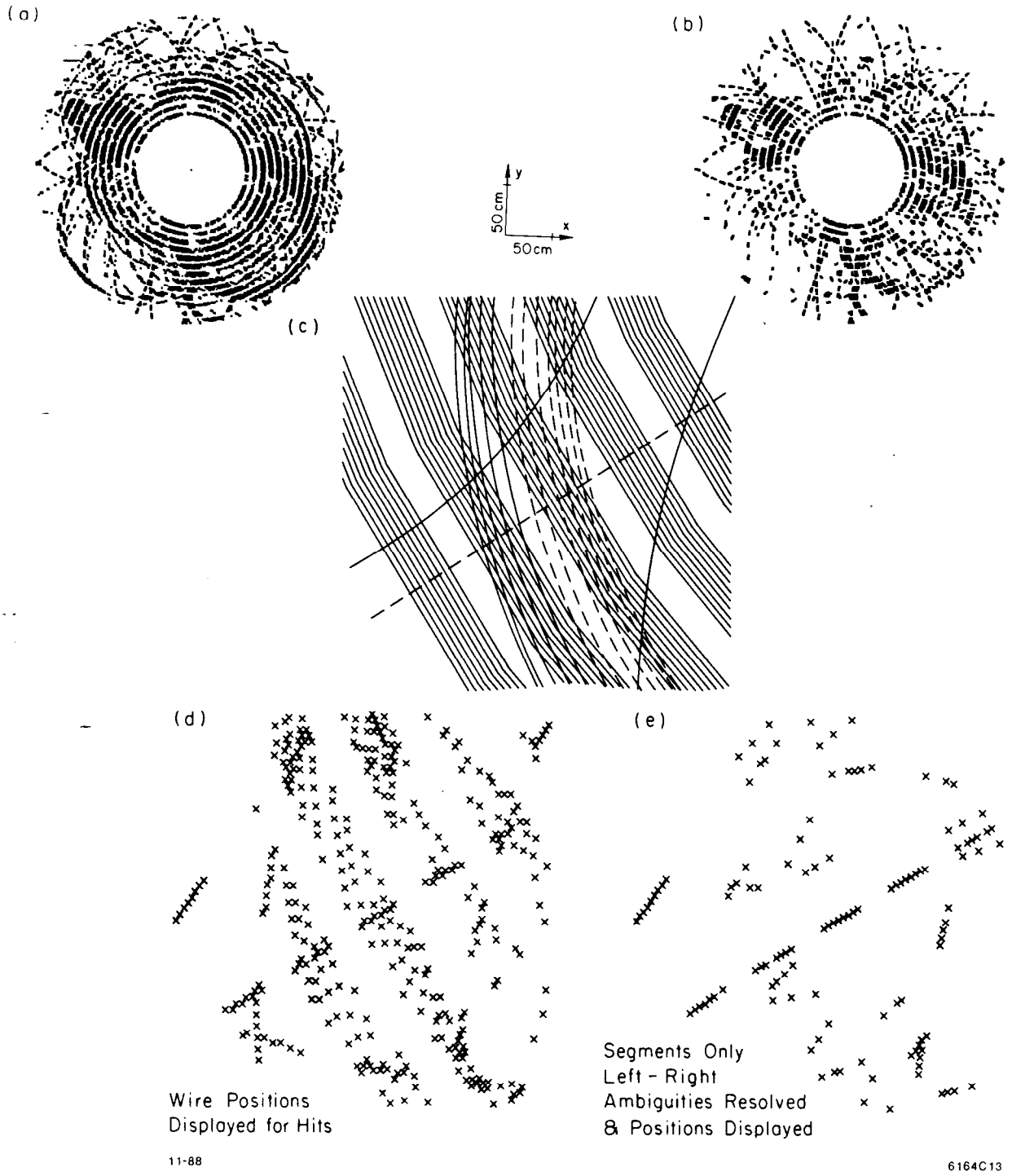

Fig. 9. (a) All of the digitizations for the Higgs event shown in fig. 7, including those from minimum bias background events. (b) Digitizations for this event which are included in track segments, as defined in the text. (c) Tracks from the original event in an enlarged region in the outer five superlayers in the region around the muon at the lower right. (d) All of the digitizations in the event in the enlarged region of (c) [the digitizations are displayed at the locations of the hit wires]. (e) Digitizations which form track segments in the enlarged region. Here, left-right ambiguities have been resolved, drift times have been converted to distances, and digitizations are displayed at the positions of closest approach of the tracks to the wires.

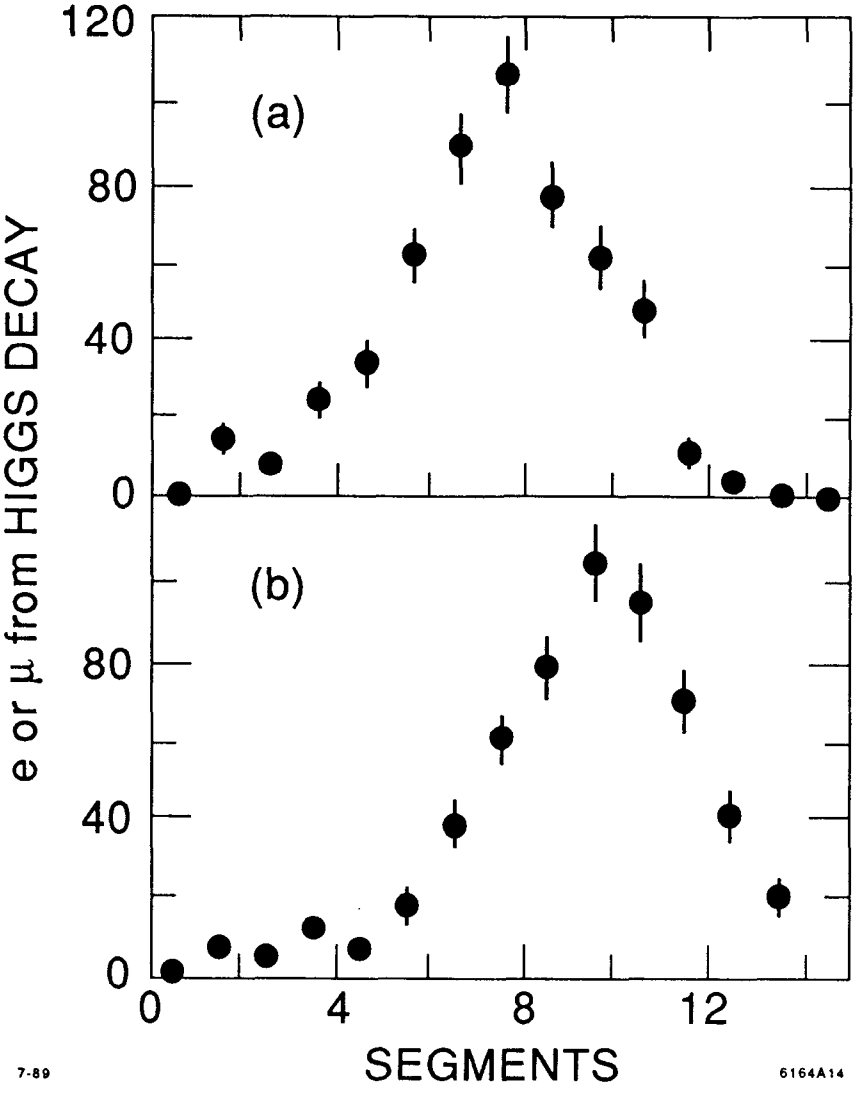

Fig. 10. (a) Distribution of the number of good segments out of 13 possible for the e's and μ's from the Higgs decays. (b) Distribution of the number of total segments (good or OK) for the leptons from the Higgs decay.

4. CONCLUSIONS

We have shown that an SSC tracking system design based on a pattern recognition strategy of finding track segments in superlayers appears to provide a powerful means of finding tracks in complex SSC events, even in an environment of multiple events from several bunch crossings. So far, detailed simulations have verified the concepts developed over several years for SSC tracking detectors. An algorithm for finding track segments such as that described here could be used in the trigger for high-p_T

tracks. Depending on the effects on the physics analyses, we might envision making this requirement at the processor level, reading out only the hits that form track segments or even just the segments themselves.

We will apply similar procedures to the simulation of radial wire chambers. Two major conceptual questions arise:

1. How can the coordinate along a radial wire be found? Do we need to use crossed planes of wires to resolve the ambiguities?

2. Can high-p_T track segments for the trigger be found quickly using radial wire chambers?

Wire chamber tracking systems for high luminosity ($\leq 10^{33}$ cm^{-2} s^{-1} at the SSC) pp colliders look feasible. However, wire chamber tracking systems will probably not survive at a luminosity of 5×10^{34}.

ACKNOWLEDGMENTS

We would like to thank the organizers of the Study Week and our hosts at the Universitat Autonoma de Barcelona for providing such a stimulating environment. We gratefully acknowledge the support of the U.S. Department of Energy Program for Generic Detector Research and Development for the SSC.

REFERENCES

[1] J. B. Dainton, "Gaseous Track Detectors at High Luminosity Colliders," and references therein, in these Proceedings.

[2] D. G. Cassel, G. G. Hanson *et al.*, "Report of the Central Tracking Group," in *Proceedings of the 1986 Summer Study on the Physics of the Superconducting Supercollider, Snowmass, CO*, 1986, eds. R. Donaldson and J. Marx, p. 377.

[3] G. A. Beck *et al.*, "Radial Wire Drift Chambers for the H1 Forward Track Detector at HERA: Design, Construction and Performance," *Proceedings of the Wire Chamber Conference, Vienna, Austria, February 13–17, 1989*, to be published in Nucl. Instr. and Meth.

[4] G. G. Hanson, "Report of the Wire Chamber Group," to appear in *Proceedings of the Workshop on Tracking Systems for the SSC, TRIUMF Laboratory, Vancouver, Canada, July 24–28, 1989.*

[5] G. G. Hanson, S. Mori, L. G. Pondrom, H. H. Williams *et al.*, "Report of the Large Solenoid Detector Group," in *Proceedings of the Workshop on Experiments, Detectors, and Experimental Areas for the Supercollider, Berkeley, CA*, 1987, eds. R. Donaldson and M.G.D. Gilchriese, p. 340.

[6] G. G. Hanson, B. B. Niczyporuk and A. P. T. Palounek, "Wire Chamber Requirements and Tracking Simulation Studies for Tracking Systems at the Superconducting Supercollider," *Proceedings of the Wire Chamber Conference, Vienna, Austria, February 13–17, 1989*, to be published in Nucl. Instr. and Meth., SLAC–PUB–4860.

[7] G. G. Hanson, B. B. Niczyporuk and A. P. T. Palounek, "Triggering and Data Acquisition Aspects of SSC Tracking," *Proceedings of the Workshop on Triggering and Data Acquisition for Experiments at the Supercollider, Toronto, Canada, January 16–19, 1989*, p. 55.

[8] G. G. Hanson, M. C. Gundy and A. P. T. Palounek, "Tracking with Wire Chambers at the SSC," to appear in *Proceedings of the 4th Pisa Meeting on Advanced Detectors, La Biodola, Isola d'Elba, Italy, May 21–26, 1989*, SLAC–PUB–5041.

[9] A. P. T. Palounek, "Simulating a Central Drift Chamber for a Large Solenoid Detector at the SSC," SLAC–PUB–4787.

[10] F. E. Paige and S. D. Protopopescu, "ISAJET 5.30: A Monte Carlo Event Generator for pp and $\bar{p}p$ Interactions," in *Proceedings of the 1986 Summer Study on the Physics of the Superconducting Supercollider, Snowmass, CO*, 1986, eds. R. Donaldson and J. Marx, p. 320. (The current version of ISAJET is 6.12.)

[11] R. Brun, F. Bruyant, and A. C. McPherson, *GEANT3 User's Guide*, CERN DD/EE/84–1.